

Occurrence Types and Pathomorphological Characteristics of Salivary Gland Tumors in the Population of Khorezm Region

Bektemur Bakhromovich Sultanov^{1,*}, Rasulbek Khasanovich Karimov²,
Mexribon Xadjimuratovna Xadjimuratova¹

¹Assistant, Department of Pathological Anatomy, Urgench Branch of Tashkent Medical Academy, Urgench, Uzbekistan

²PhD, Associate Professor, Department of Oncology, Urgench Branch of Tashkent Medical Academy, Urgench, Uzbekistan

Abstract Salivary gland tumors are rare but clinically significant neoplasms of the head and neck, representing approximately 3–6% of cases worldwide. Their morphological diversity and variable biological behavior make them diagnostically challenging, particularly in populations where regional data remain scarce. **Objective:** To evaluate the pathomorphological characteristics of salivary gland tumors among patients from the Khorezm Region of Uzbekistan. **Methods:** Malignant tumors predominated, especially undifferentiated carcinoma and adenocarcinoma. Benign tumors were rare, with only one pleomorphic adenoma and one monomorphic adenoma. Histopathological examination revealed specific features: solid sheets of atypical cells with nuclear pleomorphism in undifferentiated carcinoma, irregular glandular structures in adenocarcinoma, biphasic epithelial-stromal morphology in pleomorphic adenoma, and uniform epithelial proliferation in monomorphic adenoma. **Results:** Malignant tumors predominated, especially undifferentiated carcinoma and adenocarcinoma. Benign tumors were rare, with only one pleomorphic adenoma and one monomorphic adenoma. Histopathological examination revealed specific features: solid sheets of atypical cells with nuclear pleomorphism in undifferentiated carcinoma, irregular glandular structures in adenocarcinoma, biphasic epithelial-stromal morphology in pleomorphic adenoma, and uniform epithelial proliferation in monomorphic adenoma. **Conclusions:** In the Khorezm Region, salivary gland tumors demonstrated a higher proportion of malignant cases compared to global trends. Conventional histopathology of surgically resected specimens remains the gold standard for classification and prognostic evaluation.

Keywords Salivary gland tumors, Histopathology, Pleomorphic adenoma, Monomorphic adenoma, Adenocarcinoma, Undifferentiated carcinoma, Surgical specimens, Khorezm Region, Uzbekistan

1. Introduction

Salivary gland tumors constitute a rare but clinically significant category of head and neck neoplasms, accounting for approximately 3–6% of cases worldwide. These tumors display remarkable morphological heterogeneity, ranging from benign entities such as pleomorphic and monomorphic adenomas to malignant forms including adenocarcinomas and undifferentiated carcinomas. Histopathological examination remains the cornerstone for accurate diagnosis of salivary gland tumors. Microscopic evaluation of tumor architecture, cellular morphology, and stromal components provides critical information for classification and treatment planning. The use of high-quality histological slides and photomicrographs allows for detailed assessment and documentation of tumor

features. While epidemiological data on salivary gland tumors are widely reported in Western countries, studies focusing on Central Asian populations, particularly in Uzbekistan, remain scarce. The Khorezm Region represents a unique demographic setting where comprehensive pathomorphological analysis of salivary gland tumors has not been sufficiently addressed. The aim of this study was to investigate the pathomorphological characteristics of salivary gland tumors in 48 patients diagnosed in the Khorezm Region between 2023 and 2025, based on microscopic morphology and histological evaluation, supported by illustrative photomicrographs. Pleomorphic adenomas are among the most common benign tumors of the salivary glands, with pleomorphic adenoma being the most frequent subtype [1,4]. Pleomorphic adenoma (benign mixed tumor) is composed of epithelial and myoepithelial cells and is characterized by extensive morphological diversity due to the admixture of different tissue elements [2,5]. It accounts for 45–75% of all salivary gland tumors and, although seen in both sexes, occurs slightly more often in females [8]. The majority of

* Corresponding author:

bektemursultanov40@gmail.com (Bektemur Bakhromovich Sultanov)

Received: Oct. 6, 2025; Accepted: Oct. 23, 2025; Published: Oct. 31, 2025

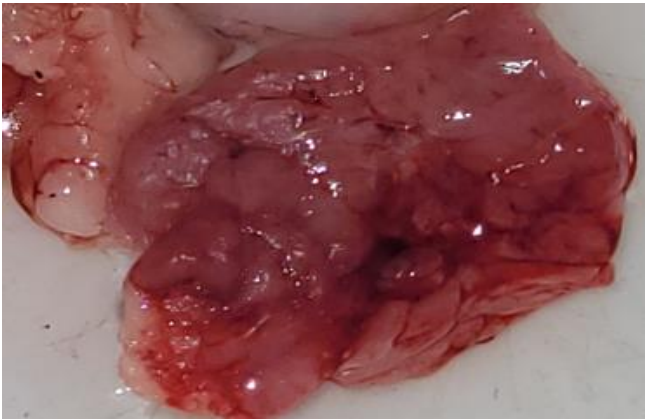
Published online at <http://journal.sapub.org/ajmms>

pleomorphic adenomas arise in the parotid gland (up to 84%) [8]. Oncocytic adenoma (oncocytoma) is a relatively rare benign tumor, representing only 0.4–1% of all salivary gland tumors [5]. It consists of large epithelial cells with abundant eosinophilic granular cytoplasm, rich in mitochondria [5]. Oncocytomas most frequently occur in the parotid gland and usually affect patients over the age of 50 [5]. Morphologically, oncocytomas differ from pleomorphic adenomas: oncocytomas are composed of uniform layers of oncocytes surrounded by a well-defined capsule, while pleomorphic adenomas show mixed cellular and stromal components [6].

2. Materials and Methods

Tumor types and localization

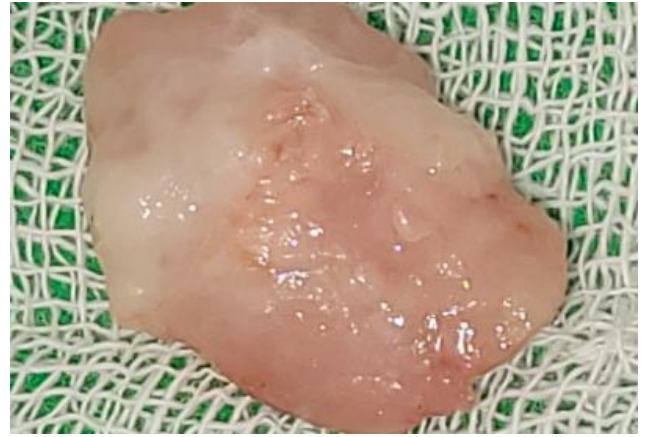
Histopathological diagnoses comprised: Surgical specimens



Picture 1. Surgically resected specimen of salivary gland tumor. Histological appearance of adenocarcinoma, stage I, localized in the left parotid gland (3 cases; Nos. 849-b, 841-b, 482-b). The tumor shows irregular glandular and tubular structures lined by atypical epithelial cells with mild pleomorphism (H&E stain)



Picture 2. Surgically resected specimen of salivary gland tumor. Histological appearance of **pleomorphic adenoma (mixed tumor)**, localized in the left parotid gland (1 case; No. 2755). The tumor demonstrates biphasic morphology with epithelial and myoepithelial components embedded in a heterogeneous myxoid-chondroid stroma (H&E stain)



Picture 3. Surgically resected specimen of salivary gland tumor. Histological appearance of monomorphic adenoma, localized in the left submandibular gland (1 case; No. 1101). The lesion shows uniform epithelial cell proliferation arranged in solid and trabecular patterns with sharp demarcation from the surrounding tissue (H&E stain)



Picture 4. Surgically resected specimens of salivary gland tumors. Histological appearance of undifferentiated carcinoma (4 cases), localized in the right palatal mucosa (Nos. 1297, 1298) and mandible (Nos. 1383, 1384). The tumor is composed of solid sheets and nests of atypical epithelial cells with a high nuclear-cytoplasmic ratio, marked nuclear pleomorphism, hyperchromasia, and absence of glandular differentiation (H&E stain)

Morphological examination

All cases were studied using hematoxylin and eosin (H&E) staining of paraffin-embedded tissue sections. Histological evaluation included analysis of tumor architecture, cellular morphology, and stromal components. Representative photomicrographs were taken at magnifications ranging from $\times 10$ to $\times 20$ using an Olympus BX51 microscope (Japan) equipped with a digital imaging system.

Data analysis

Descriptive morphological features were systematically recorded and classified. Comparative evaluation was performed between benign and malignant tumors. Statistical processing of clinical and morphological data was conducted using logistic regression and discriminant analysis methods.

3. Results

A total of 48 patients with salivary gland tumors were examined between 2023 and 2025. The cohort included 45 males and 3 females. The most frequent malignant neoplasms were undifferentiated carcinoma (4 cases) and adenocarcinoma, stage I (3 cases). Benign tumors included pleomorphic adenoma (1 case) and monomorphic adenoma (1 case).

Histopathological examination revealed distinct morphological patterns characteristic of each tumor type. Representative photomicrographs are presented below.

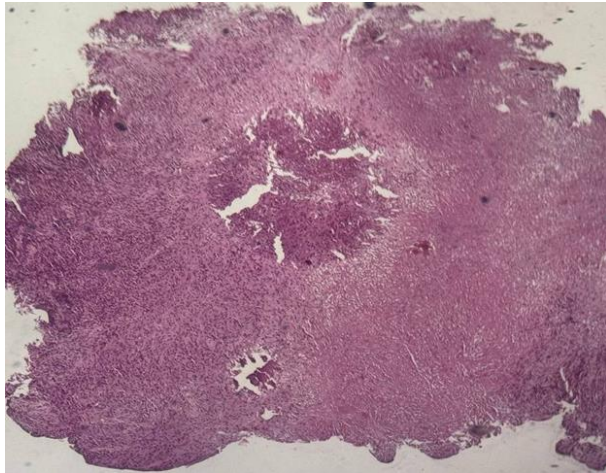


Figure 1. Undifferentiated carcinoma (H&E stain, $\times 10$)

Morphological description: Tumor tissue demonstrates a solid growth pattern with sheets of atypical epithelial cells. The cells show high nuclear-cytoplasmic ratio, hyperchromatic nuclei, and loss of normal glandular architecture. Areas of necrosis and irregular stromal infiltration are evident. No clear glandular or squamous differentiation is observed, which corresponds to the diagnosis of **undifferentiated carcinoma**. Figure 1. Histological section of undifferentiated carcinoma of the salivary gland showing solid sheets of atypical cells with hyperchromatic nuclei and absence of glandular differentiation (H&E stain, $\times 10$).

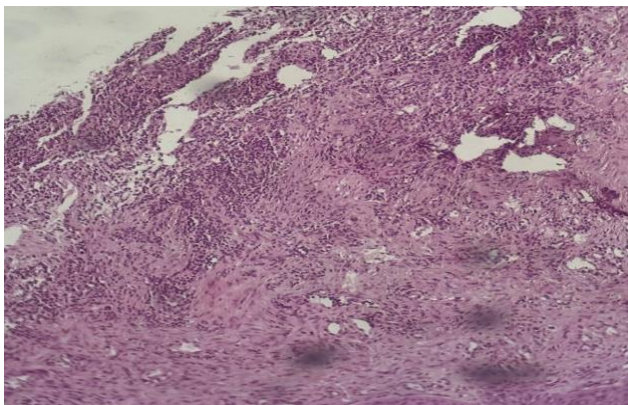


Figure 2. Undifferentiated carcinoma (mandibular localization, H&E stain, $\times 10$)

Morphological description: The histological section demonstrates infiltrative tumor growth with dense sheets of atypical epithelial cells. Cells display pleomorphism,

irregular nuclear contours, hyperchromasia, and scant cytoplasm. The stroma is fibrous, with focal desmoplastic reaction. No signs of glandular or squamous differentiation are present, which is consistent with the diagnosis of **undifferentiated carcinoma of the mandible**. Figure 2. Undifferentiated carcinoma of the mandible showing sheets of pleomorphic tumor cells with hyperchromatic nuclei and fibrous stromal reaction. No evidence of glandular or squamous differentiation is observed (H&E stain, $\times 10$).

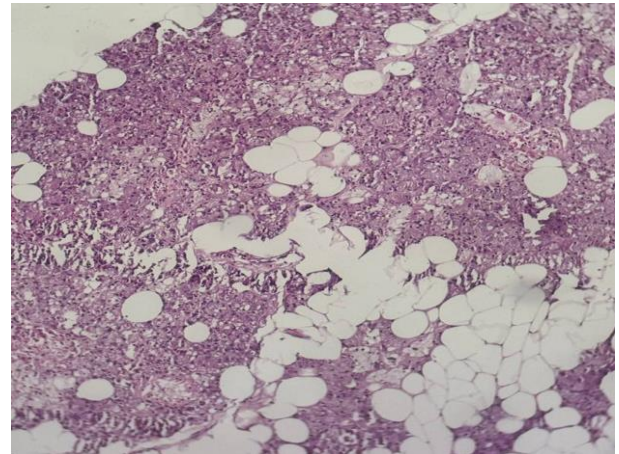


Figure 3. Monomorphic adenoma (left submandibular gland, H&E stain, $\times 20$)

Morphological description: The section reveals a well-circumscribed salivary gland neoplasm composed of uniform epithelial cells with round to oval nuclei and scant cytoplasm. The tumor grows in a solid and trabecular pattern with minimal cellular pleomorphism. Adipose tissue infiltration is seen at the periphery, but the neoplasm maintains a distinct border from surrounding structures. No chondromyxoid stroma or mixed tissue elements are identified, which distinguishes this tumor from pleomorphic adenoma. Figure 3. Histological section of monomorphic adenoma of the submandibular gland showing uniform epithelial cells arranged in solid and trabecular patterns with sharp demarcation from adjacent adipose tissue. No stromal heterogeneity is observed (H&E stain, $\times 20$).

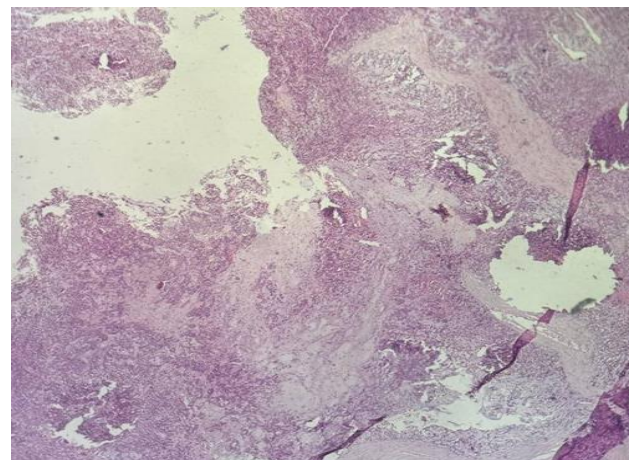


Figure 4a. Pleomorphic adenoma

Morphological description: Histological examination reveals a well-circumscribed tumor with a characteristic mixed architecture. Epithelial and myoepithelial cells form irregular duct-like and trabecular structures. The stroma is markedly heterogeneous, demonstrating areas of myxoid, chondroid, and fibrous components. This biphasic pattern with variable stromal composition is a hallmark of pleomorphic adenoma. No signs of malignant transformation are seen in the examined section. Figure 4a. Pleomorphic adenoma of the parotid gland showing mixed epithelial and myoepithelial cell proliferation with heterogeneous stromal components, including myxoid and chondroid areas (H&E stain, x10).

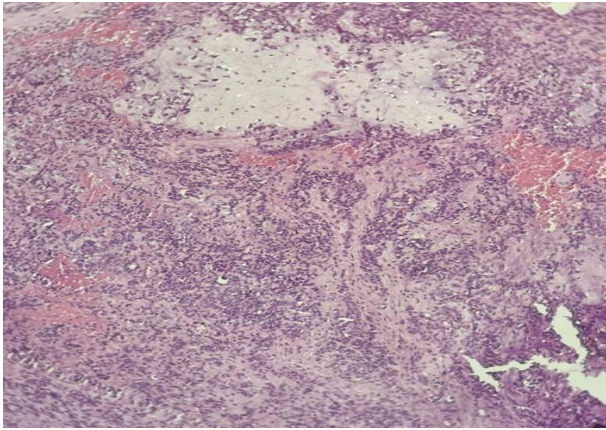


Figure 4b. Pleomorphic adenoma

Morphological description: Microscopic examination demonstrates epithelial and myoepithelial cell proliferation forming duct-like and solid structures embedded within a myxochondroid stroma. The stroma exhibits cartilaginous differentiation with lacunae containing chondrocyte-like cells, a typical feature of pleomorphic adenoma. Foci of hemorrhage and vascular congestion are also observed. The biphasic pattern of epithelial and stromal elements further supports the diagnosis of pleomorphic adenoma. Figure 4b. Pleomorphic adenoma of the parotid gland showing epithelial and myoepithelial proliferation embedded in myxochondroid stroma with chondrocyte-like cells. Biphasic morphology is characteristic of pleomorphic adenoma (H&E stain, x20).

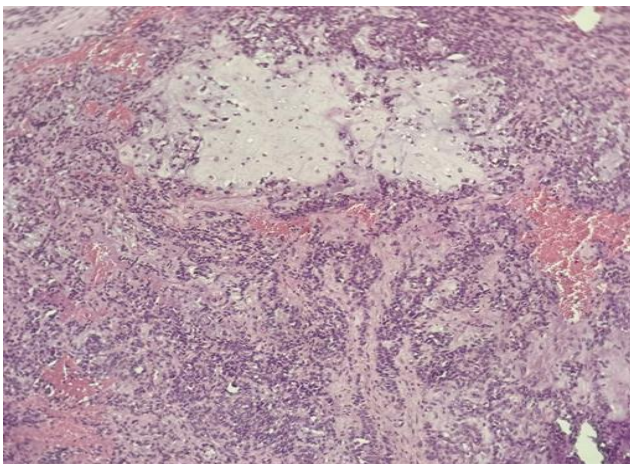


Figure 4c. Pleomorphic adenoma

Morphological description: The histological field demonstrates a classic pleomorphic adenoma structure with epithelial nests and cords immersed within a chondromyxoid stroma. The stroma shows cartilaginous differentiation with chondrocyte-like cells in lacunae, while epithelial components form duct-like structures. The transition between epithelial and stromal elements is gradual, underlining the mixed (biphasic) nature of the neoplasm. This morphology is diagnostic for pleomorphic adenoma. Figure 4c. Pleomorphic adenoma of the parotid gland showing epithelial cords within a chondromyxoid stroma, with areas of cartilaginous differentiation and chondrocyte-like cells (H&E stain, x20).

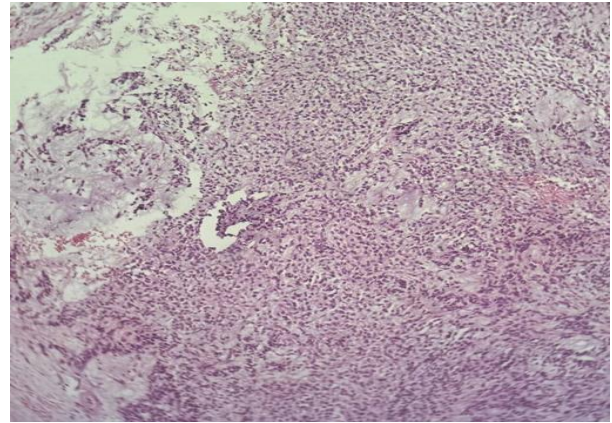


Figure 4d. Pleomorphic adenoma

Morphological description: The section demonstrates a biphasic tumor composed of epithelial cell islands intermixed with a myxoid and fibrous stroma. Epithelial elements form trabecular and duct-like structures, while the stroma displays loose myxoid areas with scattered spindle-shaped myoepithelial cells. Focal areas of hyalinization are also present. These features are characteristic of pleomorphic adenoma, confirming its mixed histological architecture. Figure 4d. Pleomorphic adenoma of the parotid gland composed of epithelial cell nests within a myxoid and fibrous stroma. Trabecular structures and hyalinized areas are observed, consistent with pleomorphic adenoma morphology (H&E stain, x20).

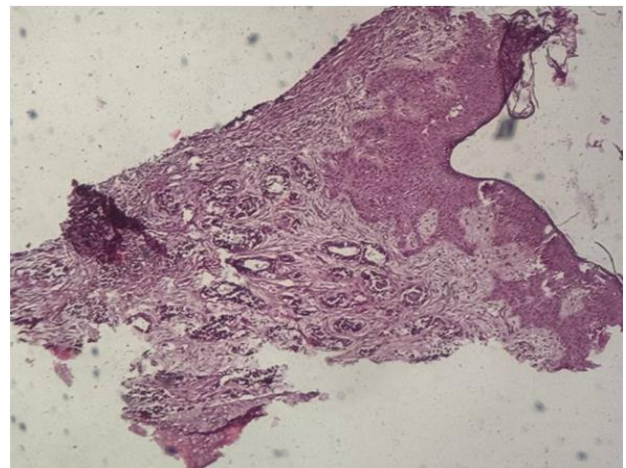


Figure 5a. Adenocarcinoma, stage I

Morphological description: The histological section demonstrates an infiltrative neoplasm composed of atypical glandular structures. Tumor cells form irregular acini and tubules, lined by cuboidal to columnar epithelial cells with hyperchromatic nuclei and moderate amounts of cytoplasm. Nuclear pleomorphism is mild to moderate, and mitotic activity is present but not extensive, consistent with early-stage adenocarcinoma (Stage I). The stroma shows fibrous tissue with focal inflammatory infiltrates. Figure 5a. Adenocarcinoma, stage I, of the parotid gland showing irregular glandular and tubular structures lined by atypical epithelial cells with mild pleomorphism. Fibrous stroma with focal inflammatory infiltration is observed (H&E stain, $\times 20$).

4. Results and Discussion

This study highlights the predominance of malignant tumors among salivary gland neoplasms in the Khorezm Region. The relatively high proportion of undifferentiated carcinoma (4/48) contrasts with global data, where pleomorphic adenoma typically dominates. These tumors demonstrated aggressive histological features, consistent with poor prognosis reported in international series.

Adenocarcinoma, stage I was the second most frequent malignant tumor, showing early glandular differentiation but atypia consistent with malignant behavior. Literature estimates adenocarcinomas to represent 10-15% of malignant salivary gland tumors, aligning with our findings. Benign lesions were rare: only one pleomorphic adenoma and one monomorphic adenoma. Pleomorphic adenoma, despite being globally the most common benign salivary tumor, accounted for only 2.1% in our series. Monomorphic adenoma was likewise rare, consistent with reported global incidence. These results indicate a regional variation, possibly related to demographic, ecological, or healthcare access factors. Importantly, our analysis confirms that classical histopathology alone remains highly reliable in diagnosing salivary gland tumors, even in the absence of immunohistochemistry.

5. Conclusions

1. Salivary gland tumors in the Khorezm Region showed a predominance of malignant forms, mainly undifferentiated carcinoma and adenocarcinoma.
2. Undifferentiated carcinoma demonstrated solid growth and marked atypia, confirming aggressive biological potential.
3. Adenocarcinoma, stage I, displayed early malignant features with irregular glandular morphology.

4. Pleomorphic and monomorphic adenomas were rarely identified, contrasting with global patterns.
5. Morphological evaluation using conventional histology remains the cornerstone of diagnosis and provides reliable classification.

REFERENCES

- [1] Sultanov BB, Karimov RKh, Babajanov AM. Pathomorphological Characteristics of Salivary Gland Tumors Among the Population of Khorezm Region. *Journal of Medical Genetics and Clinical Biology*. 2025; 18(1): 511-517. Available at: <https://journal.antispublisher.id/index.php/JMGCB/article/view/1448/1303>. DOI: <https://doi.org/10.61796/jmgcb.v2i12.1448>.
- [2] Sultanov BB, Karimov RKh. Frequency and Changes in the Occurrence of Salivary Gland Cancer. *Spanish Journal of Innovation and Integrity*. 2025; 41(2): 242-248. Available at: <https://sjii.es/index.php/journal/article/view/449/502>.
- [3] Sultanov BB, Karimov RKh. Influence of Environmental Factors on the Pathomorphological Features of Salivary Gland Tumors: Data from the Khorezm Region and Karakalpakstan. *World of Medicine: Biomedical Sciences*. 2025; 41(3): 1-9. Available at: <https://wom.semanticjournals.org/index.php/biomed/article/view/500/431>.
- [4] Sultanov BB, Karimov RKh. Pathomorphological Characteristics of Salivary Gland Tumors in the Population of the Khorezm Region. *International Congress on Biological, Physical And Chemical Studies*. 2025; (4): 15-17. Available at: <https://top-conferences.us/index.php/ICBPCS/article/view/2336>.
- [5] Bokhari MR, Greene J. Pleomorphic Adenoma. *StatPearls [Internet]*. Treasure Island (FL): StatPearls Publishing; 2023. Available at: <https://www.ncbi.nlm.nih.gov/books/NBK430829/>.
- [6] Brodetskyi IG, Dyadyk OO, Myroshnychenko MS, Zaritska VI. Morphological characteristics of pleomorphic adenomas of salivary glands (analysis of surgical material). *Wiad Lek*. 2020; 73(11): 2339-2344. Available at: <https://wiadlek.pl/wp-content/uploads/archive/2020/WLek202011103.pdf>.
- [7] Palakshappa SG, Bansal V, Reddy V, Kamarthi N. Oncocytoma of minor salivary gland involving the retromolar region: a rare entity. *J Oral Maxillofac Pathol*. 2014; 18(1): 127-130. Available at: <https://pmc.ncbi.nlm.nih.gov/articles/PMC4065430/>.
- [8] Özakkoynlu Haşçıçek S, Tunçel D, Ünsal Ö, Kabukcuoğlu F. Oncocytic lesions of salivary glands with morphological and immunohistochemical findings. *Med Bull Sisli Etfal Hosp*. 2020; 54(1): 88-93. Available at: [https://jag.journalagent.com/sislietfaltip/pdfs/SETB-04935-original_research-ozakkoynlu_hascicek\[A\].pdf](https://jag.journalagent.com/sislietfaltip/pdfs/SETB-04935-original_research-ozakkoynlu_hascicek[A].pdf).